

# Theoretical and experimental study on PMD-supported transmission using polarization diversity in coherent optical OFDM systems

W. Shieh, X. Yi, Y. Ma, and Y. Tang

ARC Special Research Centre for Ultra-Broadband Information Networks and National ICT Australia  
Department of Electrical and Electronics Engineering  
The University of Melbourne, Melbourne, VIC 3010, Australia  
e-mail: [w.shieh@ee.unimelb.edu.au](mailto:w.shieh@ee.unimelb.edu.au)

**Abstract:** In this paper, we conduct theoretical and experimental study on the PMD-supported transmission with coherent optical orthogonal frequency-division multiplexing (CO-OFDM). We first present the model for the optical fiber communication channel in the presence of the polarization effects. It shows that the optical fiber channel model can be treated as a special kind of multiple-input multiple-output (MIMO) model, namely, a two-input two-output (TITO) model which is intrinsically represented by a two-element Jones vector familiar to the optical communications community. The detailed discussions on variations of such coherent optical MIMO-OFDM (CO-MIMO-OFDM) models are presented. Furthermore, we show the first experiment of polarization-diversity detection in CO-OFDM systems. In particular, a CO-OFDM signal at 10.7 Gb/s is successfully recovered after 900 ps differential-group-delay (DGD) and 1000-km transmission through SSMF fiber without optical dispersion compensation. The transmission experiment with higher-order PMD further confirms the resilience of the CO-OFDM signal to PMD in the transmission fiber. The nonlinearity performance of PMD-supported transmission is also reported. For the first time, nonlinear phase noise mitigation based on receiver digital signal processing is experimentally demonstrated for CO-OFDM transmission.

©2007 Optical Society of America

**OCIS codes:** (060.0060) Fiber optics and optical communications; (060.1660) Coherent communications; (060.5060) Phase modulation

---

## References and links

1. C. Poole, R. Tkach, A. Chraplyvy, and D. Fishman, "Fading in lightwave systems due to polarization-mode dispersion," *IEEE Photon. Technol. Lett.* **3**, 68-70 (1991).
2. W. Shieh, and C. Athaudage, "Coherent optical orthogonal frequency division multiplexing," *Electron. Lett.* **42**, 587-589 (2006).
3. W. Shieh, "PMD-supported coherent optical OFDM systems," *IEEE Photon. Technol. Lett.* **19**, 134-136 (2006).
4. N. Cvijetic, L. Xu, and T. Wang, "Adaptive PMD Compensation using OFDM in Long-Haul 10Gb/s DWDM Systems," in *Optical Fiber Communication Conference and Exposition and The National Fiber Optic Engineers Conference*, Technical Digest, (Optical Society of America, Washington, DC, 2007), Paper OTuA5.
5. I. B. Djordjevic, "PMD compensation in fiber-optic communication systems with direct detection using LDPC-coded OFDM," *Opt. Express* **15**, 3692-3701 (2007).
6. C. Laperle, B. Villeneuve, Z. Zhang, D. McGhan, H. Sun, and M. O'Sullivan, "Wavelength division multiplexing (WDM) and Polarization Mode Dispersion (PMD) performance of a coherent 40Gbit/s dual-polarization quadrature phase shift keying (DP-QPSK) transceiver," in *Optical Fiber Communication Conference and Exposition and The National Fiber Optic Engineers Conference*, Technical Digest, (Optical Society of America, Washington, DC, 2007), Paper PDP16.

7. G. Charlet1, J. Renaudier, M. Salsi, H. Mardoyan, P. Tran, and S. Bigo, "Efficient mitigation of fiber impairments in an ultra-long haul transmission of 40Gbit/s Polarization-multiplexed data, by digital processing in a coherent receiver," in *Optical Fiber Communication Conference and Exposition and The National Fiber Optic Engineers Conference*, Technical Digest, (Optical Society of America, Washington, DC, 2007), Paper PDP17.
8. W. Shieh, X. Yi, and Y. Tang, "Transmission experiment of multi-gigabit coherent optical OFDM systems over 1000 km SSMF fiber," *Electron. Lett.*, **43**, 183-185 (2007).
9. S. L. Jansen, I. Morita, N. Takeda, and H. Tanaka, "20-Gb/s OFDM transmission over 4,160-km SSMF enabled by RF-Pilot tone phase noise compensation," in *Optical Fiber Communication Conference and Exposition and The National Fiber Optic Engineers Conference*, Technical Digest, (Optical Society of America, Washington, DC, 2007), Paper PDP15.
10. N. Gisin, and B. Huttner, "Combined effects of polarization mode dispersion and polarization dependent losses in optical fibers," *Opt. Commun.* **142**, 119-125 (1997).
11. H. Bolcskei, D. Gesbert, and A. J. Paulraj, "On the capacity of OFDM-based spatial multiplexing systems," *IEEE Trans. Commun.* **50** (2), 225-34 (2002).
12. Y. Tang, W. Shieh, X. Yi, R. Evans, "Optimum design for RF-to-optical up-converter in coherent optical OFDM systems," *IEEE Photon. Technol. Lett.* **19**, 483 - 485 (2007).
13. W. Shieh, "On the second-order approximation of PMD," *IEEE Photon. Technol. Lett.* **12**, 290-292 (2000).
14. H. Bulow, "System outage probability due to first- and second-order PMD," *IEEE Photon. Technol. Lett.* **10** (5), 696-698 (1998).
15. W. Shieh, R. S. Tucker, W. Chen, X. Yi, and G. Pendock, "Optical performance monitoring in coherent optical OFDM systems," *Opt. Express* **15**, 350-356 (2007).
16. K.P. Ho, and J.M. Kahn, "Electronic compensation technique to mitigate nonlinear phase noise," *J. of Lightwave Technol.* **22**, 779-783 (2004).
17. K. Kikuchi, M. Fukase, and S. Kim, "Electronic post-compensation for nonlinear phase noise in a 1000-km 20-Gbit/s optical QPSK transmission system using the homodyne receiver with digital signal processing," in *Optical Fiber Communication Conference and Exposition and The National Fiber Optic Engineers Conference*, Technical Digest, (Optical Society of America, Washington, DC, 2007), PaperOTuA2.

## 1. Introduction

Polarization-mode dispersion (PMD) has long been considered as the fundamental barrier to high-speed optical transmission. For conventional direct-detection single-carrier systems, the impairment induced by a constant differential-group-delay (DGD) scales with the square of the bit rate, resulting in drastic PMD degradation for high speed transmission systems [1]. We recently proposed a multi-carrier modulation format, called coherent optical orthogonal frequency-division multiplexing (CO-OFDM) to combat fiber dispersion [2]. We also introduced the concept of PMD-supported optical transmission for which the PMD does not pose impairment to the CO-OFDM signal [3]. In particular, the PDL impairment mitigation and nonlinearity reduction are suggested as potential benefits of PMD-supported transmission. The theoretical fundamentals and associated signal processing are discussed in [3], but there has been no experimental proof for the PMD mitigation theory. PMD mitigation is also discussed with simulation in the context of incoherent optical OFDM (IO-OFDM) [4-5]. Experimental demonstration of the PMD mitigation in single-carrier systems has recently been reported by several groups [6-7]. In the field of multi-carrier CO-OFDM long haul transmission, the first transmission experiment has been reported for 1000 km SSMF transmission at 8 Gb/s [8], and more CO-OFDM transmission experiment have rapidly been reported by S. Jensen et. al. for 4160 km SSMF transmission at 20 Gb/s [9]. However, the above two CO-OFDM transmission experiments required manual polarization tracking in the receiver, which is impractical for the field application. It is thus desirable to have polarization-diversity scheme by which the performance is independent of the incoming polarization without a need for a dynamically-controlled polarization-tracking device. In this paper, we conduct both theoretical and experimental study on the PMD-supported CO-OFDM transmission. We first present the model for the optical fiber communication channel in the presence of polarization effects. It shows that the optical fiber channel model can be treated as a two-input two-output (TITO) MIMO model, which is intrinsically represented by a two-element Jones vector familiar to the optical communication community. The detailed

discussions on various optical MIMO-OFDM schemes are also presented. Furthermore, by using polarization-diversity detection and OFDM signal processing on the two-element OFDM information symbols at the receiver, we show experimentally record PMD tolerance with CO-OFDM transmission. In particular, a CO-OFDM signal at 10.7 Gb/s is successfully recovered after 900 ps differential-group-delay (DGD) and 1000-km transmission through SSMF fiber without optical dispersion compensation. The transmission experiment with higher-order PMD further confirms the immunity of the CO-OFDM signal to PMD in the transmission fiber. The nonlinearity performance of PMD-supported transmission is also reported. For the first time, nonlinear phase noise mitigation based on the receiver digital signal processing is experimentally demonstrated for CO-OFDM transmission. We note that the demonstration is performed without any additional optical polarization controller before the receiver. The significance of this work is two-fold. First we present a feasible solution to reuse old fiber which may have large PMD values. Secondly, the PMD resilience for CO-OFDM is shown to be independent of data rate [2], and our experimental demonstration can be potentially scaled to a higher speed system, only limited to the state-of-art electronic signal processing capability. It is important to note that in this paper, we define PMD-supported transmission as the transmission with two attributes, (i) resilience to PMD, and (ii) no need for any optical polarization tracking device before the receiver. We will use ‘PMD-supported’ and the two aforementioned attributes interchangeably in the paper.

## 2. Theoretical model for coherent optical MIMO-OFDM signals in the presence of polarization effects

It is well-known that optical fiber can support two polarization modes. The propagation of an optical signal is influenced by the polarization effects including polarization mode coupling and polarization dependent loss (PDL). This paper will focus on analytical derivation of the linear effects including polarization mode dispersion (PMD), PDL and chromatic dispersion (CD). The numerical study of the nonlinear polarization effects on CO-OFDM transmission will be reported in a separate submission.

Similar to the single-polarization OFDM signal model [2], the transmitted OFDM time-domain signal,  $s(t)$  is described using Jones vector given by

$$s(t) = \sum_{i=-\infty}^{+\infty} \sum_{k=-\frac{1}{2}N_{sc}+1}^{\frac{1}{2}N_{sc}} \vec{c}_{ik} \Pi(t - iT_s) \exp(j2\pi f_k(t - iT_s)) \quad (1)$$

$$s(t) = \begin{pmatrix} s_x \\ s_y \end{pmatrix}, \quad \vec{c}_{ik} = \begin{pmatrix} c_{ik}^x \\ c_{ik}^y \end{pmatrix} \quad (2)$$

$$f_k = \frac{k-1}{t_s} \quad (3)$$

$$\Pi(t) = \begin{cases} 1, & (-\Delta_G < t \leq t_s) \\ 0, & (t \leq -\Delta_G, t > t_s) \end{cases} \quad (4)$$

where  $s_x$  and  $s_y$  are the two polarization components for  $s(t)$  in the time-domain,  $\vec{c}_{ik}$  is the transmitted OFDM information symbol in the form of Jones vector for the  $k$ th subcarrier in the  $i$ th OFDM symbol,  $c_{ik}^x$  and  $c_{ik}^y$  are the two polarization components for  $\vec{c}_{ik}$ ,  $f_k$  is the frequency for the  $k$ th subcarrier,  $N_{sc}$  is the number of OFDM subcarriers,  $T_s$ ,  $\Delta_G$ , and  $t_s$  are the OFDM symbol period, guard interval length and observation period respectively. The Jones vector  $\vec{c}_{ik}$  is employed to describe generic OFDM information symbol regardless of any polarization configuration for the OFDM transmitter. In particular, the  $\vec{c}_{ik}$  encompasses

various modes of the polarization generation including single-polarization, polarization multiplexing and polarization-modulation, as they all can be represented by a two-element Jones vector  $\vec{c}_{ik}$ . The different scheme of polarization modulation for the transmitted information symbol is automatically dealt with in initialization phase of OFDM signal processing by sending known training symbols.

We select a guard interval long-enough to handle the fiber dispersion including PMD and CD. This timing margin condition is given by

$$\frac{c}{f^2} |D_t| \cdot N_{sc} \cdot \Delta f + DGD_{\max} \leq \Delta_G \quad (5)$$

where  $f$  is the frequency of the optical carrier,  $c$  is the speed of light,  $D_t$  is the total accumulated chromatic dispersion in units of ps/pm,  $N_{sc}$  is the number of the subcarriers,  $\Delta f$  is the subcarrier channel spacing, and  $DGD_{\max}$  is the maximum budgeted differential-group-delay (DGD), which is about 3.5 times of the mean PMD to have sufficient margin.

Following the same procedure as [2], assuming using long-enough symbol period, we arrive at the received symbol given by

$$\vec{c}'_{ki} = e^{j\phi_i} \cdot e^{j\Phi_D(f_k)} \cdot T_k \cdot \vec{c}_{ki} + \vec{n}_{ki} \quad (6)$$

$$T_k = \prod_{l=1}^N \exp \left\{ \left( -\frac{1}{2} j \cdot \vec{\beta}_l \cdot f_k - \frac{1}{2} \vec{\alpha}_l \right) \cdot \vec{\sigma} \right\} \quad (7)$$

$$\Phi_D(f_k) = \pi \cdot c \cdot D_t \cdot f_k^2 / f_{LD1}^2 \quad (8)$$

where  $\vec{c}'_{ki} = \begin{pmatrix} c'^x_{ki} & c'^y_{ki} \end{pmatrix}^t$  is the received information symbol in the form of the Jones vector for the  $k$ th subcarrier in the  $i$ th OFDM symbol,  $\vec{n}_{ki} = \begin{pmatrix} n^x_{ki} & n^y_{ki} \end{pmatrix}^t$  is the noise including two polarization components,  $T_k$  is the Jones matrix for the fiber link,  $N$  is the number of PMD/PDL cascading elements represented by their birefringence vector  $\vec{\beta}_l$  and PDL vector  $\vec{\alpha}_l$  [10],  $\vec{\sigma}$  is the Pauli matrix vector [10],  $\Phi_D(f_k)$  is the phase dispersion owing to the fiber chromatic dispersion (CD) [2], and  $\phi_i$  is the OFDM symbol phase noise owing to the phase noises from the lasers and RF local oscillators (LO) at both the transmitter and receiver [2].  $\phi_i$  is usually dominated by the laser phase noise.

Equations similar to (6)-(8) have been reported in [3]. However, the discussion was focussed on the single-polarization modulation at the transmit end. We point out here that (6) in essence shows a MIMO model relating the two outputs  $c'^x_{ik}$  and  $c'^y_{ik}$  to the two inputs  $c^x_{ik}$  and  $c^y_{ik}$ . Such a MIMO model has been widely investigated to improve the performance of wireless systems [11]. We consider the discussion of the coherent optical MIMO OFDM channel model (6) as one of the main contributions of this paper, which will be illustrated in the subsequent paragraphs.

### 3. Coherent optical MIMO-OFDM models

In the context of the multiple-input multiple-output (MIMO) system, the architecture of CO-OFDM system is divided into four categories according to the number of the transmitters and receivers used in the polarization dimension. The detailed discussion is given as follows:

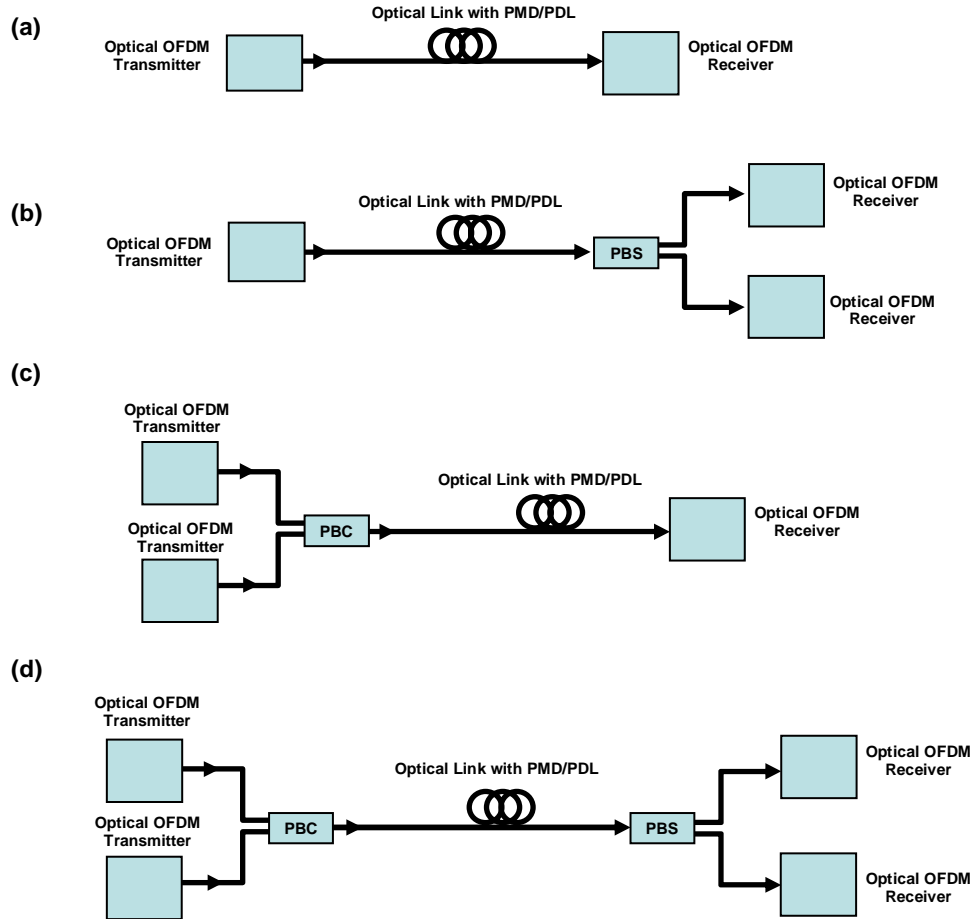


Fig. 1. Variations of coherent optical MIMO OFDM (CO-MIMO-OFDM) models: (a) single-input single-output (SISO), (b) single-input two-output (SITO), (c) two-input single-output (TISO), and (d) two-input two-output (TITO). The optical OFDM transmitter includes RF OFDM transmitter and OFDM RF-to-optical up-converter, and the optical OFDM receiver includes OFDM optical-to-RF down-converter and RF OFDM receiver. PBC/S: Polarization Beam Combiner/Splitter.

### 3.1 Single-input single-output (SISO)

As shown in Fig. 1(a), one optical OFDM transmitter and one optical OFDM receiver are used for CO-OFDM transmission. The optical OFDM transmitter includes an RF OFDM transmitter and an OFDM RF-to-optical up-converter whereas the optical OFDM receiver includes an OFDM optical-to-RF down-converter, and an RF OFDM receiver [2, 12]. The architectures of the OFDM up/down converters are thoroughly discussed in [12]. For instance, in the direct up/down conversion architecture, an optical I/Q modulator can be used as the up-converter and a coherent optical receiver including an optical  $90^\circ$  hybrid and a local laser can be used as the down-converter [12].

The SISO configuration is susceptible to the polarization mode coupling in the fiber, analogous to the multi-path fading impairment in SISO wireless systems [11]. A polarization controller is needed before the receiver to align the input signal polarization with the local oscillator polarization [8-9]. More importantly, in the presence of large PMD, due to the polarization rotation between subcarriers, even the polarization controller will not function well. This is because there is no uniform subcarrier polarization that the local receiver laser

can align its polarization with. Subsequently, coherent optical SISO-OFDM is susceptible to polarization-induced fading and should not be implemented in the field application.

### 3.2 Single-input two-output (SITO)

As shown in Fig. 1(b), at the transmit end, only one optical OFDM transmitter is used. However, compared with the SISO system, there are two optical OFDM receivers employed, one for each polarization. The receiver shown in Fig. 1(b) is the so-called polarization-diversity receiver as discussed in both single-carrier [7] and multi-carrier systems [3]. As such, there is no need for optical polarization control. Furthermore, the impact of PMD on CO-OFDM transmission is simply a subcarrier polarization rotation, which can be easily treated through channel estimation and constellation reconstruction [3]. Therefore, coherent optical SITO-OFDM is resilient to PMD when the polarization-diversity receiver is used. Most importantly, the introduction of PMD in the fiber link in fact will improve the system margin against PDL-induced fading [3], analogous to the scenario for which the delay spread channel improves the wireless MIMO system performance [11].

### 3.3 Two-input single-output (TISO)

As shown in Fig. 1(c), at the transmit end, two optical OFDM transmitters are used, one for each polarization. However, at the receive end, only one optical OFDM receiver is used. This transmitter configuration is called polarization-diversity transmitter. By configuring the transmitted OFDM information symbols properly, the CO-OFDM transmission can be performed without a need for a polarization controller at the receiver. One possible transmission scheme is shown as follows: At the transmitter, the same OFDM symbol is repeated in two consecutive OFDM symbols with orthogonal polarizations. For instance, this can be done by simply turning on and off the two transmitters alternately in each OFDM symbol. Formally the transmitted OFDM information symbols for the two consecutive OFDM symbols are written as

$$\bar{c}_{(2i-1)k} = a_{ik} \begin{pmatrix} 0 \\ 1 \end{pmatrix} \quad (9)$$

$$\bar{c}_{(2i)k} = a_{ik} \begin{pmatrix} 1 \\ 0 \end{pmatrix} \quad (10)$$

It can be easily shown that the received Jones vector information symbol  $\vec{c}'_{ik}$  by combining two consecutive OFDM symbols (number  $2i-1$  and number  $2i$ ) is equivalently given by

$$\vec{c}'_{ik} = a_{ik} T_k \begin{pmatrix} 1 \\ 0 \end{pmatrix} \quad (11)$$

It can be seen from Eq. 11, the polarization-diversity transmitter can also achieve PMD-supported transmission, namely, PMD-resilience and no need for polarization tracking. This seems to show that TISO has the same performance as SITO. However, in the TISO scheme, the same information symbol is repeated in two consecutive OFDM symbols, and subsequently the electrical and optical efficiency is reduced by half, and the OSNR requirement is doubled, compared with the SITO scheme.

### 3.4 Two-input two-output (TITO)

As shown in Fig. 1(d), both a polarization-diversity transmitter and a polarization-diversity receiver are employed in the TITO scheme. Firstly, in such a scheme, because the transmitted OFDM information symbol  $\bar{c}_{ik}$  can be considered as polarization modulation or polarization multiplexing, the capacity is thus doubled compared with SITO scheme. As the impact of the PMD is to simply rotate the subcarrier polarization, and can be treated with channel

estimation and constellation reconstruction, and therefore the doubling of the channel capacity will not be affected by PMD. Secondly, due to the polarization-diversity receiver employed at the receive end, TITO scheme does not need polarization tracking at the receiver.

From the above analysis in the framework of CO-MIMO-OFDM models, except the SISO scheme, all the other schemes are capable of PMD-supported transmission. However, as we have discussed, TISO scheme has intrinsic penalties in spectral efficiency (electrical and optical) and OSNR sensitivity. Consequently, SITO and TITO OFDM transmission are the preferred configurations. For the remainder of the paper, we will show the experimental demonstration using SITO architecture.

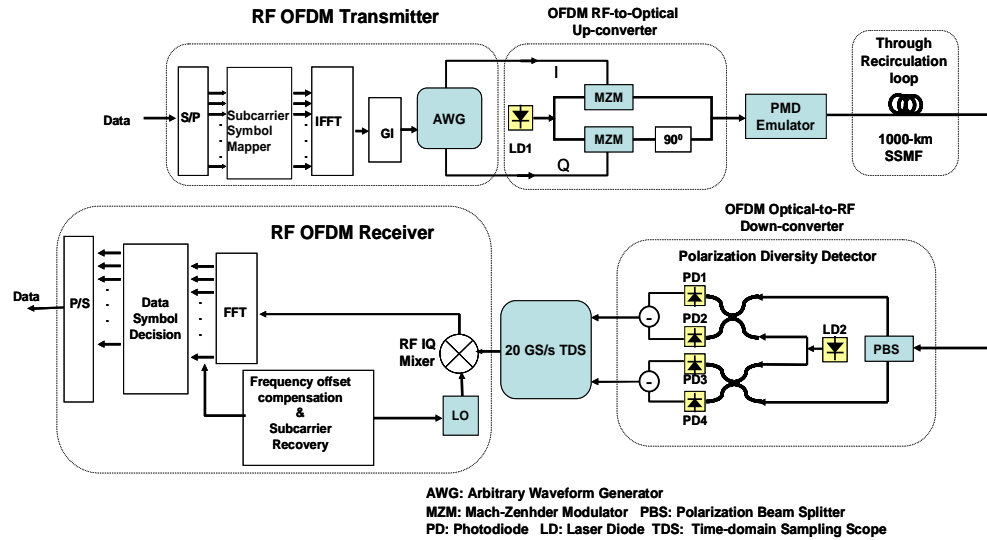


Fig. 2. Experimental setup for PMD-supported CO-OFDM transmission

#### 4. Experimental setup for PMD-supported CO-OFDM transmission

Figure 2 shows the experimental setup for verifying the PMD-supported CO-OFDM systems equivalent of SITO MIMO-OFDM architecture. The OFDM signal is generated by using a Tektronix Arbitrary Waveform Generator (AWG) as an RF OFDM transmitter. The time domain waveform is first generated with a Matlab program including mapping  $2^{15}-1$  PRBS into corresponding 77 subcarriers with QPSK encoding within multiple OFDM symbols, which are subsequently converted into time domain using IFFT, and inserted with guard interval (GI). The number of OFDM subcarriers is 128 and guard interval is 1/8 of the observation period. Only middle 87 subcarriers out of 128 are filled, from which 10 pilot subcarriers are used for phase estimation. This filling is to achieve tighter spectral control by over-sampling and should not be confused with the selective carrier filling due to channel fading. The BER performance is measured using all the 77 data bearing channels. The OFDM digital waveform of  $s(t)$  (Eq. 1) is complex value. Its real and imaginary parts are uploaded into the AWG operated at 10 GS/s, and two-channel analogue signals each representing the real and imaginary components of the complex OFDM signal are generated synchronously. The so-generated OFDM waveform carries 10.7 Gb/s data. These two signals are fed into I and Q ports of an optical I/Q modulator respectively, to perform direct up-conversion of OFDM baseband signals from RF domain to optical domain [12]. The optical OFDM signal from the I/Q modulator is first inserted into a home-built PMD emulator, and then fed into a recirculation loop which includes one span of 100 km SSMF fiber and an EDFA to compensate the loss. We would like to stress that this is the first experimental demonstration of the direct up-conversion with an optical I/Q modulator for CO-OFDM system. The

advantages of such a direct up-conversion scheme are (i) the required electrical bandwidth is less than half of that of intermediate frequency (IF) counterpart, and (ii) there is no need for an image-rejection optical filter [12]. The launch power into each fiber span is set at -8 dBm to avoid the nonlinearity, and the received OSNR is 14 dB after 1000 km transmission. At the receive end, the polarization-diversity detection is employed. The output optical signal from the loop is first split into two polarizations, each fed into an OFDM optical-to-RF down-converter that includes a balanced receiver and a local laser. The two RF signals for the two polarizations are then input into a Tektronix Time Domain-sampling Scope (TDS) and acquired synchronously. The RF signal traces corresponding to the 1000-km transmission are acquired at 20 GS/s and processed with a Matlab program as an RF OFDM receiver. The RF OFDM receiver signal processing involves (1) FFT window synchronization using Schmidl format to identify the start of the OFDM symbol, (2) software down-conversion of the OFDM RF signal to base-band by a complex pilot subcarrier tone, (3) phase estimation for each OFDM symbol, (4) channel estimation in terms of Jones vector and Jones Matrix, and (5) constellation construction for each carrier and BER computation. The major improvements over previous CO-OFDM experimental demonstrations [8-9] are that, (i) an optical IQ modulator is used for direct up-conversion to significantly reduce the electrical bandwidth, and (ii) the polarization diversity detection is used to eliminate the need for an optical polarization controller before the coherent receiver.

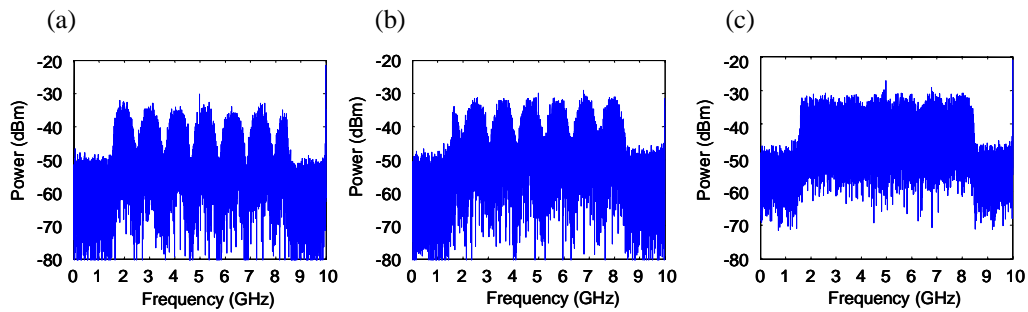


Fig. 3. (a) and (b) The RF spectra for two polarization components, and (c) the overall RF spectra

## 5. Measurement results and discussion on PMD tolerance

Figures 3(a) and 3(b) show RF spectra for the two polarization components at the output of the two balanced receivers. This is for a CO-OFDM signal which has traversed 900 ps DGD and 1000 km SSMF fiber. The spectra are obtained by performing FFT on the signal traces from the coherent detector acquired with the TDS. The periodic power fluctuation of the RF spectra with the period of 1.09 GHz represents the polarization rotation cross the entire OFDM spectrum. This agrees with the 900 ps DGD used in the experiment. Fig. 3(c) shows the summation of the two power spectra, which effectively recovers the power spectrum for a single-polarization OFDM signal. This signifies that despite the fact that the polarization of each OFDM subcarrier is rotated, but the overall energy for the two polarization components is conserved.

The RF OFDM signal (as shown in Figs. 3(a) and 3(b)) is down-converted to baseband by simply multiplying a complex residual carrier tone in software, eliminating a need for a hardware RF LO. This complex carrier tone can be supplied with the pilot symbols or pilot subcarriers. The down-converted baseband signal is segmented into blocks of 400 OFDM symbols with the cyclic prefix removed, and the individual subcarrier symbol in each OFDM symbol is recovered by using FFT.

The receiver signal processing procedure for PMD-supported system has been thoroughly discussed in [3]. The associated channel model after removing the phase noise  $\phi_i$  is given by



$$\vec{c}_{ki}'^p = H_k \vec{c}_{ki} + \vec{n}_{ki}^p \quad (12)$$

where  $\vec{c}_{ki}'^p$  is the received OFDM information symbol in a Jones vector for  $k$ th subcarrier in the  $i$ th OFDM symbol, with the phase noise removed,  $H_k = e^{j\Phi_D(f_k)} \cdot T_k$  is the channel transfer function, and  $\vec{n}_{ki}^p$  is the random noise.

The expectation values for the received phase-corrected information symbols  $\vec{c}_{ki}'^p$  are obtained by averaging over a running window of 400 OFDM symbols. The expectation values for 4 QPSK symbols are computed separately by using received symbols  $\vec{c}_{ki}'^p$ , respectively. An error occurs when a transmitted QPSK symbol in particular subcarrier is closer to the incorrect expectation values at the receiver.

Figure 4 shows the BER performance of the CO-OFDM signal after 900 ps DGD and 1000-km SSMF transmission. The optical power is evenly launched into the two principal states of the PMD emulator. The measurements using other launch angles show insignificant difference. Compared with the back-to-back case, it has less than 0.5 dB penalty at the BER of  $10^{-3}$ . We would like to stress that the DGD of 900 ps is the largest DGD tolerance for 10 Gb/s systems to the best of our knowledge. The magnitude of the PMD tolerance is shown to be independent of the data rate [3]. Therefore we expect the same PMD tolerance in absolute magnitude will hold for 40 Gb/s if faster ADC/DACs are available at 20 GS/s and above.

Each OFDM subcarrier can be considered as a flat channel experiencing a local first-order DGD. Since the first-order DGD does not present any impairment to the CO-OFDM signal as shown in Fig. 4, it is easy to show neither does the higher-order PMD. This is in sharp contrast to the conventional single-carrier systems where the second-order/higher-order PMD impairment becomes significant at large PMD [13-14]. However, to have a convincing proof of the PMD-supported transmission, we construct a higher-order PMD by inserting a 110 ps DGD emulator into the recirculation loop, and subsequently the output signal of 1000-km simulates a 10-stage PMD cascade, equivalent to a mean PMD over 300 ps. The emulator obviously does not cover all the PMD states of a mean PMD of 300 ps. We do not intend to experimentally prove a satisfactory performance for every PMD realization. Instead, we randomly change the polarization in the fiber and record the BER degradation after transmission. Fig. 5 shows the BER fluctuation for 100 random realizations of high PMD states. The BER is initially set to be  $10^{-3}$  without PMD. These realizations are shown to have high DGD along with large higher-order PMD. Despite that, it can be seen in Fig. 5 that the BER shows insignificant degradation.

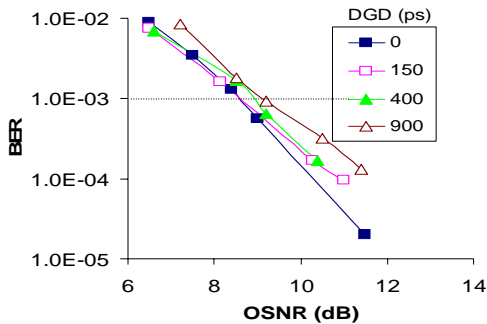


Fig. 4. BER performance of a CO-OFDM signal

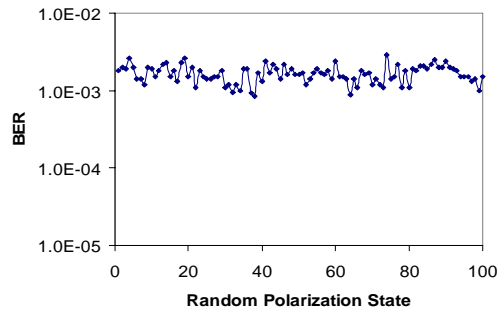


Fig. 5. BER variation as a function of PMD state

## 6. Nonlinearity performance of PMD-supported CO-OFDM transmission

The discussion so far is limited to a launch power of -8 dBm where the nonlinearity is insignificant. As any transmission systems, there exists an optimal launch power beyond which the system Q starts to decrease as the input power increases. It is of interest to identify the optimal launch power and the achievable Q for the PMD-supported system. We perform an experimental nonlinearity analysis for the PMD-supported transmission using the setup in Fig. 2. The measurement is conducted for a 10.7 Gb/s CO-OFDM signal passing through 900 ps DGD and 1000 km SSMF transmission. Fig. 6 shows the measured system Q as a function of the launch power (the curve with square). It can be seen that the optimal power is about -3.5 dBm with an optimal Q of 15.6 dB. Because of the limited number of OFDM symbols processed in the experiment, the Q factor from direct bit-error-ratio (BER) measurement is limited to 12 dB. Beyond that, a monitoring approach based upon the electrical SNR is used to estimate the Q factor (Eqs. 6-8 in [15]), namely, the Q factor shown in Fig. 6 is the monitored Q. Specifically, as in [15], we define the Q factor estimated by using the electrical SNR as monitored Q, and the Q factor obtained by direct actual bit-error-ratio (BER) as calculated Q. Furthermore, we find that at high launch powers the monitored Q deviates from the calculated Q whereas at the low launch powers, the monitored Q agrees with the calculate Q. In particular, at the launch power of 2.7 dBm, the monitored Q is 11.1 dB whereas the calculated actual Q is 9.2 dB, about 2 dB over estimation of Q in high nonlinear regime.

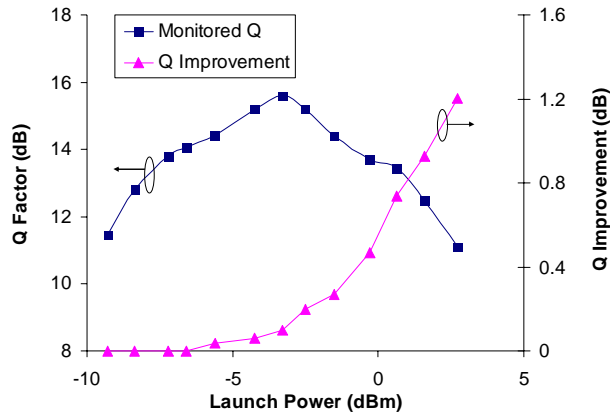


Fig. 6. System performance as a function of launch power. The curve with square is for the monitored Q factor without nonlinearity mitigation. The curve with triangle is for the monitored Q improvement with nonlinearity mitigation.

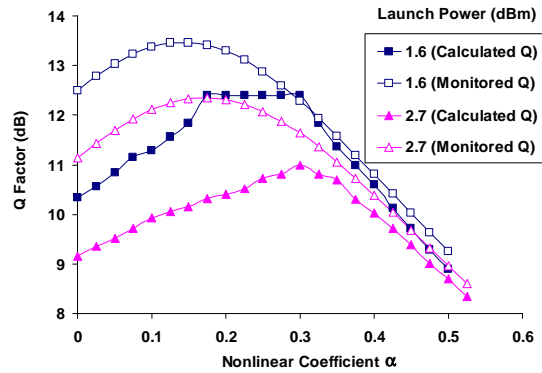


Fig. 7. System performance as a function of the nonlinear coefficient  $\alpha$  used in the receiver-based digital signal processing. The data are shown for both monitored Q and calculated (actual) Q.

The nonlinearity due to high launch power can be partially mitigated through receiver digital signal processing. The receiver-based nonlinearity reduction through digital processing has been proposed and demonstrated for single-carrier systems [16-17]. Similar to the analysis in [16], the OFDM time domain signal at the receiver  $s(t)$  can be expressed as

$$s(t) = \begin{pmatrix} s_x \\ s_y \end{pmatrix} = s_0(t) \exp(j\phi_{NL}) \quad (13)$$

$$\phi_{NL} = NL_{eff} \gamma |s|^2 = \beta I_0 |\tilde{s}|^2 = \alpha |\tilde{s}|^2, \quad |s|^2 \equiv (|s_x|^2 + |s_y|^2) \quad (14)$$

where  $s_{x/y}$  is the x/y component of the received optical signal,  $\phi_{NL}$  is the nonlinear phase noise,  $N$  is the number of spans,  $s_0(t)$  is the optical field with the optical nonlinearity removed,  $L_{eff}/\gamma$  is the effective length/nonlinear coefficient of the fiber,  $|s|^2 \equiv (|s_x|^2 + |s_y|^2)$  is the total time-varying optical signal power,  $I_0 = \langle |s|^2 \rangle$  is the average of the received optical power, and  $|\tilde{s}|^2 \equiv |s|^2 / I_0$  is the normalized received signal power,  $\beta \equiv NL_{eff} \gamma$  is the lumped nonlinearity coefficient,  $\alpha \equiv \beta I_0$  is a unitless and different representation of the nonlinear coefficient. The receiver signal processing is as follows. At the signal acquisition and initialization phase, an optimal  $\beta$  is estimated, for instance, based upon BER minimization. Then the nonlinearity mitigated field  $s_0(t)$  is obtained as

$$s_0(t) = s(t) \exp(-j\beta |s(t)|^2) \quad (15)$$

$s_0(t)$  is subsequently used for OFDM digital processing to recover data. This phenomenological nonlinear coefficient  $\beta$  is estimated without knowing what the detailed dispersion map of the fiber link is. Therefore, we expect (15) is an approximation and the nonlinear phase noise impact is only partially removed.

The curve with triangle in Fig. 6 shows the improvement of the monitored Q as a function of the launch power after the nonlinear phase noise compensation (15). It shows that the monitored Q can be improved by as much as 1 dB at high launch powers. Because of the significant disparity between the monitored Q and calculated Q values, we conduct the nonlinearity mitigation performance for both the monitored Q and the calculated Q, as a function of the  $\alpha$  parameter at high launch powers of 1.6 dBm and 2.7 dBm. It can be seen that for the launch power of 1.6 dBm (curve with solid square), the improvement of the calculated Q is more than 2 dB, and the optimal  $\alpha$  coefficient is about 0.25. The flat top shape of the curve is a result of the best BER that can be achieved by a limited number of OFDM symbols. Similarly, at the launch power of 2.7 dBm, the improvement of the calculated Q is about 2 dB, and the optimal  $\alpha$  coefficient is about 0.3. The 2 dB Q improvement is significant, considering only very small additional computation complexity needed to perform the nonlinear phase mitigation (15). This 2 dB Q improvement can be also translated into 2 dB dynamic range improvement for the launch power. Fig. 6 also shows that the optimal  $\alpha$  coefficient (or  $\beta$  coefficient) is different for the monitored Q and the calculated

Q, indicating that the calculated Q (or BER) should be used for optimal nonlinear phase noise mitigation. We note that this is the first experimental demonstration of receiver based nonlinearity mitigation in CO-OFDM systems without optical dispersion compensation.

## **7. Conclusion**

In this paper, we have conducted theoretical and experimental study on the PMD-supported transmission with coherent optical orthogonal frequency-division multiplexing (CO-OFDM). We have firstly presented the models for the optical fiber communication channel in the presence of the polarization effects. It shows that the optical fiber channel can be treated as a two-input two-output (TITO) MIMO model, which is intrinsically represented by a two-element Jones vector familiar to the optical communication community. The detailed discussions on various CO-MIMO-OFDM schemes are presented. Furthermore, by using polarization-diversity detection and OFDM signal processing on the two-element OFDM symbols at the receiver, we have shown experimentally record PMD tolerance with CO-OFDM transmission. In particular, a CO-OFDM signal at 10.7 Gb/s is successfully recovered after 900 ps DGD and 1000-km transmission through SSMF fiber without optical dispersion compensation. The transmission experiment with higher-order PMD further confirms the immunity of the CO-OFDM signal to PMD in the transmission fiber. The nonlinearity performance of PMD-supported transmission is also reported. For the first time, nonlinearity mitigation based on the receiver digital signal processing is experimentally demonstrated for CO-OFDM transmission. As a result, a 2-dB Q improvement is achieved at high launch powers.

## **Acknowledgments**

This work was supported by the Australian Research Council (ARC).